Spontaneous Human Adult Stem Cell Transformation

Daniel Rubio,[1] Javier Garcia-Castro,[1,2] María C. Martín,[3] Ricardo de la Fuente,[1] Juan C. Cigudosa,[3] Alison C. Lloyd,[4] and Antonio Bernad[1]

[1]Department of Immunology and Oncology, Centro Nacional de Biotecnología/Consejo Superior de Investigaciones Cientificas, UAM Campus de Cantoblanco; [2]Oncology Department, Hospital Universitario del Niño Jesús; [3]Cytogenetics Unit, Centro Nacional de Investigaciones Oncológicas, Madrid, Spain; and [4]Laboratory for Molecular Cell Biology, University College London, London, United Kingdom

Abstract

Human adult stem cells are being evaluated widely for various therapeutic approaches. Several recent clinical trials have reported their safety, showing them to be highly resistant to transformation. The clear similarities between stem cell and cancer stem cell genetic programs are nonetheless the basis of a recent proposal that some cancer stem cells could derive from human adult stem cells. Here we show that although they can be managed safely during the standard *ex vivo* expansion period (6-8 weeks), human mesenchymal stem cells can undergo spontaneous transformation following long-term *in vitro* culture (4-5 months). This is the first report of spontaneous transformation of human adult stem cells, supporting the hypothesis of cancer stem cell origin. Our findings indicate the importance of biosafety studies of mesenchymal stem cell biology to efficiently exploit their full clinical therapeutic potential. (Cancer Res 2005; 65(8): 3035-9)

Introduction

Stem cells are characterized by their self-renewal ability and differentiation potential (1) and can be divided into embryonic and adult stem cells. Embryonic stem cells derive from the inner mass of the blastocyst; they have the potential to give rise to an entire organism and to differentiate to all cell lineages (2). Most adult stem cells are minor populations found in adult organs; they cannot give rise to an organism and only differentiate to specific cell lineages; mesenchymal stem cells (MSC) belong to this group. MSC are multipotent cells with many potential clinical applications due to their capacity to be expanded *ex vivo* and to differentiate into several lineages, including osteocytes, chondrocytes, myocytes, and adipocytes. MSC have been isolated from bone marrow, cartilage, and adipose tissue and all show similar morphologic and phenotypic characteristics (3). Stem cells and cancer stem cells share certain features such as self-renewal and differentiation potential. Cancer stem cells have been identified and characterized in several tumor types, including acute myeloid leukemia, breast cancer, and glioblastoma (1).

Human cells have two control points that regulate their life span *in vitro*, the senescence and crisis phases. Senescence is associated with moderate telomere shortening and is characterized by cell cycle arrest and positive β-galactosidase staining at pH 6 (4). If cells bypass this stage, they continue to grow until telomeres become critically short and cells enter crisis phase, characterized by generalized chromosome instability that provokes mass apoptosis (5). Human cells immortalize at low frequency and seem resistant to spontaneous transformation. Here we report that MSC in long-term cultures immortalize at high frequency and undergo spontaneous transformation.

Materials and Methods

Isolation of adipose tissue–derived mesenchymal stem cell. Samples of discarded adipose tissue from eight pediatric and two adult non-oncogenic surgical interventions were maintained in HBSS medium (4°C) and processed within 6 hours. After extensive washing with PBS, samples were minced and digested with 1 mg collagenase *P* (Roche, Indianapolis, IN)/0.5 g sample/mL DMEM (37°C, 1 hour). Enzyme activity was inhibited by adding DMEM plus 10% heat-inactivated FCS. Samples were clarified by sedimentation (600 × *g*, 5 minutes, room temperature), the resulting cell suspension filtered through a 40 mm^2 nylon filter (Becton Dickinson, San Jose, CA), plated onto tissue culture plastic (10^3 cells/cm^2), allowed to adhere (24 hours), and washed twice with PBS (10 mL). Adipose tissue–derived MSC from C57BL/6 and CD1 mice were isolated using the same method.

Cell culture. Human and murine MSC were cultured (37°C, 5% CO_2) in MSC medium (DMEM plus 10% FCS), 2 mmol/L glutamine, 50 μg/mL gentamicin and passaged when they reached 85% confluence. Cells were treated with 0.5% trypsin plus 0.2% EDTA (5 minutes), washed with culture medium, sedimented (600 × *g*, 10 minutes, room temperature), and plated (5×10^3 cells/cm^2) in MSC medium.

Cell differentiation. Cells plated as above were allowed to adhere (24 hours); culture medium was then replaced with specific differentiation-inductive medium. For adipogenic differentiation, cells were cultured in MEM plus 10% FCS, 0.5 mmol/L 3-isobutyl-1-methylxanthine, 0.5 mmol/L hydrocortisone, 1 mmol/L dexamethasone, 200 mmol/L indomethacin, and 50 μg/mL gentamicin for 2 weeks. Differentiated cell cultures were stained with Oil Red O (Amresco, Salon, OH). For osteogenic differentiation, cells were cultured in MEM plus 10% FCS, 0.1 mmol/L dexamethasone, 50 mmol/L ascorbate-2-phosphate, 10 mmol/L β-glycerophosphate, and 50 μg/mL gentamicin for 2 weeks. Differentiated cell cultures were stained with Alizarin Red S (Sigma, St. Louis, MO).

Fluorescence-activated cell sorting analysis. Cells were analyzed in an EPICS XL-MCL cytometer (Coulter Electronics, Hialeah, FL); 10^4 cells were routinely analyzed. Antibodies were precalibrated to determine optimal concentration. Cell cycle stage was determined with the DNA-Prep Reagent Kit (Coulter Electronics).

Retroviral transduction. Murine and human MSC were transduced with retroviral supernatants (4 hours; Genetrix, Madrid, Spain) in 8 μg/mL polybrene. After incubation, cells were washed twice with PBS and incubated in fresh MSC medium. Enhanced green fluorescent protein expression was analyzed by fluorescence-activated cell sorting 48 hours after transduction.

Karyotype analysis. Metaphases were prepared from methanol/acetic acid (3:1)–fixed cells. Slides were hybridized by spectral karyotyping (Applied Spectral Imaging, Carlsbad, CA). Images were acquired with an SD300

Note: Supplementary data for this article are available at Cancer Research Online (http://canres.aacrjournals.org/).

Requests for reprints: Javier Garcia-Castro, Department of Immunology, Centro Nacional de Biotechnologia/Consejo Superior de Investigaciones Cientificas, UAM Campus de Cantoblanco, Darwin, 3 E-28049 Madrid, Spain. Phone: 34-915854656; Fax: 34-913720493; E-mail: igarciac.hnjs@salud.madrid.org.

Spectra cube (Applied Spectral Imaging) on a Zeiss Axioplan microscope with a SKY-1 optical filter (Chroma Technology, Rockingham, VT). At least 20 metaphase cells were analyzed from each MSC or transformed mesenchymal cell (TMC) preparation. Breakpoints were assigned based on 4′,6-diamidino-2-phenylindole banding and G-banded karyotype.

Western blot. After cell extract fractionation by 10% SDS-PAGE, followed by transfer to polyvinylidene difluoride membranes, c-myc levels were monitored by incubation (1:200, 1 hour, room temperature) with the sc-40 mouse monoclonal antibody (Santa Cruz Biotechnology, Santa Cruz, CA) and peroxidase-labeled goat anti-mouse antibody (Dako, Glostrup, Denmark; 1 hour), and developed using enhanced chemiluminescence (Amersham, Buckinghamshire, United Kingdom). p16 (Oncogene, Uniondale, NY) levels were monitored using the same protocol. A mouse anti-human tubulin monoclonal antibody (Sigma; 1:5,000, 1 hour, room temperature) was used to confirm loading equivalence.

Telomerase activity. Telomerase activity was analyzed using the TRAPeze Detection Kit (Chemicon, Temecula, CA). PCR products were separated in a 12.5% polyacrylamide gel. After drying, the gel was developed by autoradiography.

***In vivo* tumorigenesis.** Female BALB/c-SCID mice were sublethally γ-irradiated (2.5 Gy) and infused i.v. with 10^6 cells. Animals were killed when they were ill and their organs extracted for further analyses.

Immunohistochemistry. Organs were fixed with 4% PFA (1 hour), included in OCT (Jung) and 6- to 8-μm sections prepared on a cryostat (Leica). Sections were stained with anti-human mitochondrial monoclonal antibody (NeoMarkers, Fremont, CA), followed by biotinylated goat anti-mouse antibody (Vector Laboratories, Burlingame, CA; 1 hour, room temperature), developed with the avidin-biotin complex Kit (Vectastain) and mounted using Depex (Serva).

***In vivo* angiogenesis.** Female BALB/c-SCID mice were inoculated s.c. with 500 μL Matrigel (Becton Dickinson) containing 5×10^4 cells, 100 ng/mL vascular endothelial growth factor (VEGF; R&D Systems, Minneapolis, MN), and 64 units/mL heparin (Sigma). Mice were killed 6 days after infusion, Matrigel removed and fixed with 4% PFA (1 hour), included in OCT, and sectioned as above. Sections were stained with Cy3-coupled anti-GFP antibody and rhodamine-phalloidin (both from Molecular Probes, Eugene, OR; 1 hour, room temperature). Images were captured using a fluorescence microscope.

***In vitro* vascular endothelial growth factor quantification.** Cells were plated (12.5×10^3 cells/cm^2); after 72 hours, supernatants were collected and VEGF quantified using an anti-human VEGF ELISA (R&D Systems).

Results and Discussion

We isolated 10 MSC samples from human adipose tissue, which we maintained in long-term *in vitro* culture. Adipose tissue–derived MSC showed typical fibroblast-like morphology (Fig. 1*A*); they expressed cell surface antigens CD13, CD90, and CD105, and low CD106 levels (Fig. 1*B*), characteristic of adipose-derived MSC (6). To confirm the differentiation potential of these cells, we used specific differentiation-inducing stimuli in MSC cultures, which yielded osteocytes (Fig. 1*C*) and adipocytes (Fig. 1*D*). The results concur with previous data using cells from processed lipoaspirate (6). Immediately after isolation, all MSC had a normal 2n karyotype (Fig. 2*B*); these cells were injected into immunodeficient animals ($n = 8$), and no signs of tumor formation were detected when mice were sacrificed after 1 to 4 months.

Cells were allowed to proliferate and subplated when they reached preconfluence. All samples entered the senescence phase ~2 months after isolation, concurring with data on other human primary cells (4). Senescence duration varied from 1 to 8 weeks, during which cells underwent cycle arrest and showed positive β-galactosidase staining at pH 6 (data not shown). All MSC isolates bypassed this crisis phase spontaneously and subsequently showed an accelerated cell cycle rate compared with presenescence MSC, in agreement with studies of cells that bypass the senescence phase spontaneously (7). Karyotype analysis showed certain differences between presenescence and post-senescence MSC samples. Although all cells had a normal karyotype after isolation, at least 30% of post-senescence MSC presented trisomy of chromosome 8 (Fig. 2*B*). We injected these cells into immunodeficient mice ($n = 14$) using the protocol applied for presenescence MSC and obtained comparable results; none of the mice showed signs of tumor formation when analyzed, in some cases after 3 months.

Post-senescence MSC cultures continued to grow until they reached crisis phase (Fig. 2*A*). Cell cycle analysis showed generalized chromosome instability, as described (ref. 8; Supplementary Fig. S1*A*). Of the samples tested, 50% escaped crisis spontaneously and continued to proliferate. During this process,

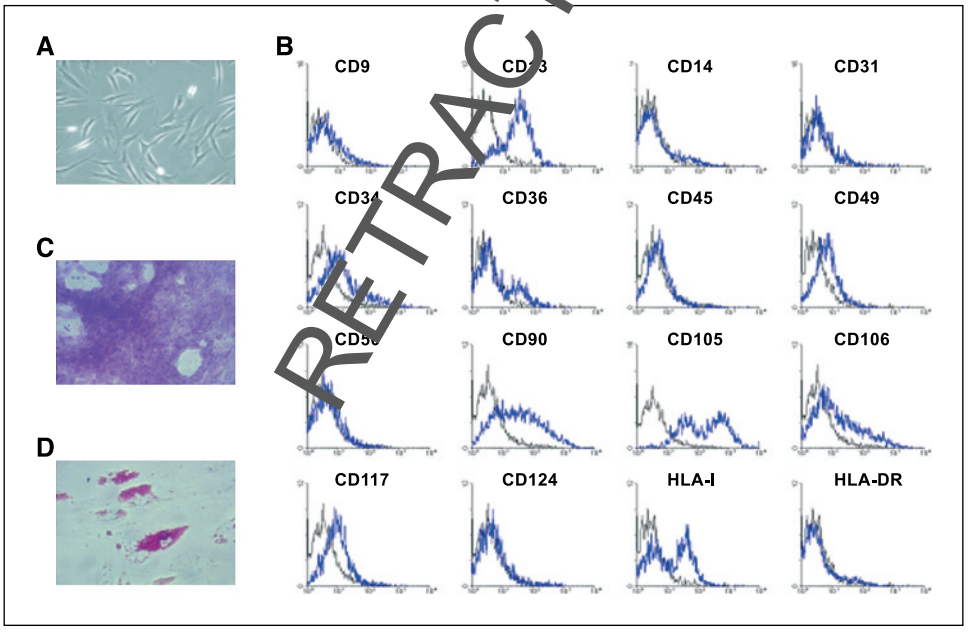

Figure 1. MSC characterization. *A,* MSC morphology after isolation. *B,* fluorescence-activated cell sorting analysis of MSC surface markers. *C,* osteogenic differentiation of Alizarin Red–stained MSC. *D,* adipogenic differentiation of Oil Red O–stained MSC.

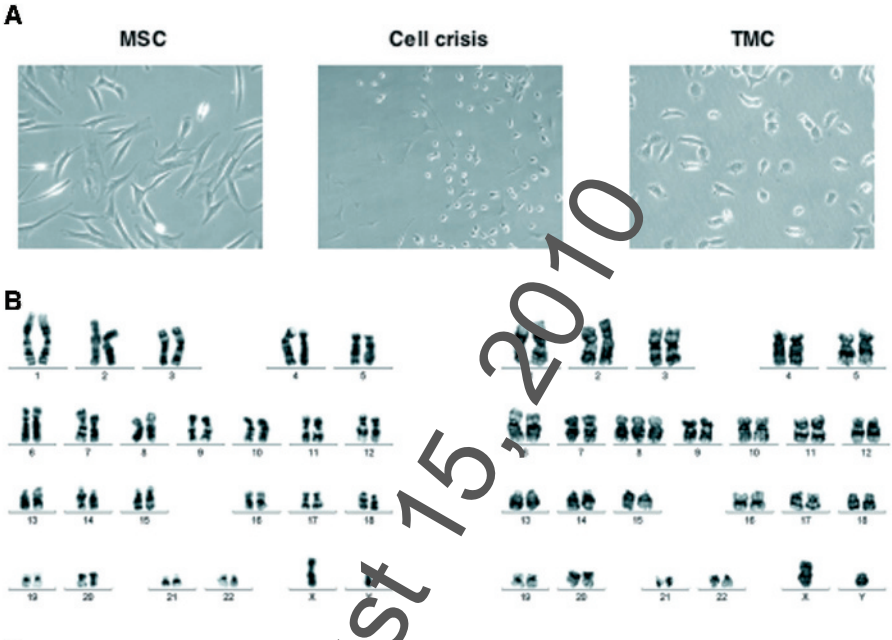

D

Sample	MSC-TMC transition	Post-senescence MSC	TMC karyotype
14	YES	46,XY, der(5)t(5;5)(p15;?), der(11)t(3;11)(?;q25)	81,XXYYYY, der(5)t(5;5)(p15;?), der(11)t(3;11)(?;q25)
14 EGFP	YES	ND	45,XO, der(5)t(5;5)(p15;?), der(11)t(3;11)(?;q25)
14 EGFP2	YES	47,XY i(8)	45,X0,t(2;2)(p12;q37), der(5)t(5;5)(p15;?), i(8)(q10),der(11)t(3;11)(?;q25)
16	NO	47,XY i(8)	—
16 EGFP	YES	47,XY i(8)	45,XO, der(5)t(5;5)(p15;?), der(11)t(3;11)(?;q25)
16 EGFP2	YES	ND	45,XY, der(5)t(5;5)(p15;?), der(11)t(3;11)(?;q25)
21	NO	46,XY	—
23	NO	46,XY	—
31	NO	ND	—
32	NO	ND	—
C57/BL6	YES	ND	ND
CD1	YES	ND	ND

Figure 2. TMC characterization. *A,* evolution of MSC morphology during *in vitro* culture (*left* to *right*): MSC, cell crisis phase, and TMC. *B,* G-banded karyotype of a normal MSC line, 46,XY (*left*) and of a precrisis MSC line, 47,XY i(8) (*right*). *C,* G-banded karyotype of a TMC line, 45,X0, t(2;2)(p12;q37),der(5)t(5;5)(p15;?),i(8)(q10), der(11)t(3;11)(?;q25) (*left*); *right,* spectral karyotyping of the TMC line as in (*B*). Chromosome abnormalities (*small numbers at right of each chromosome*). *D,* characteristics associated with long-term MSC culture, including MSC-to-TMC transition and karyotypes. *ND,* not determined.

the MSC phenotype changed from an elongated spindle shape to a small, compact morphology (Fig. 2*A*). Cell cycle analysis showed an increase in the percentage of S-phase cells in postcrisis cultures, with reduced duplication time compared with the precrisis population (Supplementary Fig. S1*A*). Cells showed chromosome instability during and after crisis (ref. 9 and Supplementary Fig. S1*A*), as well as an altered phenotype. Postcrisis cells down-regulated membrane markers CD34, CD90, and CD105 (Supplemenrtary Fig. S1*B*). As cells lost contact inhibition and grew in semisolid agar (data not shown), both characteristic features of tumor cells (10), we termed them TMCs.

Karyotype analysis of TMC samples showed trisomy, tetraploidy, and/or chromosome rearrangement (Fig. 2*C*). These changes were nonrandom and consistent in the isolates, including a recurring translocation between chromosomes 3 and 11 and intrachromosomal rearrangement of chromosome 5, with occasional presence of an isochromosome 8 (Fig. 2*D*). Genetic instability in human tumors usually involves chromosome alterations; in particular, sarcomas often show a disease-specific pattern of cytogenetic alterations (11) similar to these TMC. We searched the abnormal karyotypic regions for genes that might be modulated between presenescence and post-senescence MSC, as well as TMC. c-*myc*, a chromosome 8 oncogene that affects cell cycle progression and gene expression modifications (12), was affected in at least 30% of post-senescence MSC and in some TMC. Presenescence MSC had very low c-myc levels, which increased in MSC during and after senescence. TMC also showed higher c-myc levels than presenescence MSC (Fig. 3*A*). The data suggest that c-myc overexpression may play a role in senescence bypass and contribute to TMC transformation.

Another potential target gene was that encoding telomerase, the enzyme responsible for elongating telomeres at chromosome ends, which normally shorten at each cell division. This gene is located on the short arm of chromosome 5, a region affected in all our TMC. We measured telomerase activity in presenescence and post-senescence MSC and in TMC; neither presenescence nor post-senescence MSC showed detectable telomerase activity, whereas telomerase activity in all TMC samples was similar to telomerase-positive control cells (Fig. 3*B*). These data concur with reports linking crisis bypass and cell immortalization with telomerase expression or telomerase-independent mechanisms of telomere maintenance (13).

Due to its importance in senescence and tumor formation, we examined p16 levels in presenescence and post-senescence MSC and in TMC. Post-senescence MSC expressed lower p16 levels than the presenescence samples. In the TMCs, p16 levels could not be detected (Fig. 3*C*).

We injected TMC into immunodeficient mice, all of which showed signs of illness by 4 to 6 weeks post-injection (lordosis, cachexia, respiratory distress, and hair loss), when their organs were analyzed. We found tumors in all TMC-injected mice (n = 38), in nearly all organs. In contrast, we detected no signs of illness or tumor formation in mice inoculated with presenescence or post-senescence MSC. Some mice received enhanced green fluorescent protein–transduced TMC, allowing fluorescence detection of tumor aggregates in organs (Fig. 4*A-H*); tumor nodules coincided with fluorescent staining (Fig. 4*I-J*). To confirm the TMC origin of the tumors, we did immunohistochemical analysis using an anti-human mitochondria monoclonal antibody; positive staining (Fig. 4*K-L*) confirmed that the TMC had become tumorigenic. Cells isolated from TMC-inoculated mouse tumor nodules and expanded *in vitro* showed the morphology and chromosome instability described above (data not shown). Although it is a very infrequent phenomenon, spontaneous immortalization of human cells has been reported (14); here we show not only that MSC can immortalize at high frequency but that with further *ex vivo* culture, 50% of the samples underwent spontaneous transformation, a process not previously described for human cells.

As VEGF is involved in the development of many tumor types (15), we compared its expression in presenescence MSC and in TMC cultures in ELISA and found higher VEGF levels in TMC (Supplementary Fig. S2*A*). In an *in vivo* functional assay based on s.c. injection of cells mixed with Matrigel, we observed size and color differences between MSC/Matrigel and TMC/Matrigel samples (Supplementary Fig. S2*B*). At 6 days post-injection, TMC/Matrigel had a greater volume and a hemorrhagic appearance, suggestive of a more complex vascular network. This was confirmed by histologic analysis of the TMC/Matrigel, which showed defined vessels (Supplementary Fig. S2*C*) surrounded by tumor nodules (Supplementary Fig. S2*D*). These tumor aggregates, derived from s.c. injected TMC, confirmed the findings of the i.v. TMC injection assay.

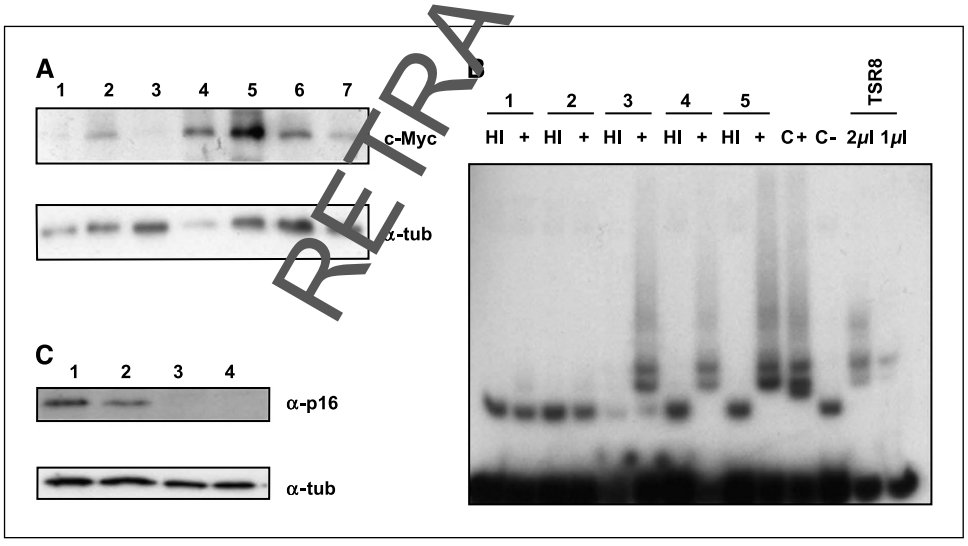

Figure 3. Genes differentially expressed in MSC versus TMC. *A,* c-myc and control α-tubulin (*α-tub*) levels in presenescence MSC (*lanes 1* and *3*), senescence MSC (*lane 4*), post-senescence MSC (*lane 2*), and TMC (*lanes 5-7*). *B,* telomerase activity in presenescence MSC (*sample 1*), post-senescence MSC (*sample 2*), or TMC (*samples 3-5*). *HI,* sample heat-inactivated as negative control of telomerase activity. TSR8 oligo control supplied with the kit (*right*). *C,* p16 and control α-tubulin (*α-tub*) levels in presenescence MSC (*lane 1*), post-senescence MSC (*lane 2*), and TMC (*lanes 3* and *4*).

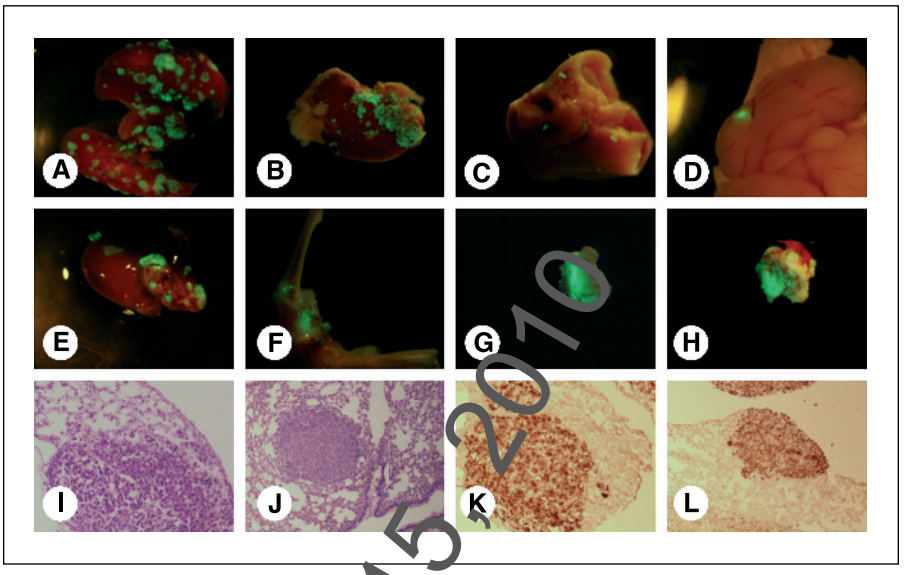

Figure 4. *In vivo* analysis of TMC. Organs extracted from mice inoculated with EGFP-TMC show fluorescent tumor nodules in (*A*) lung, (*B*) kidney, (*C*) liver, (*D*) brain, (*E*) heart, (*F*) striated muscle, (*G*) ovary, and (*H*) suprarenal gland. *I-J,* H&E staining of lung infiltrated with TMC. Tumor mass is surrounded by the parenchyma. *K-L,* peroxidase-conjugated anti-human mitochondrial monoclonal antibody staining of mouse lung infiltrated with TMC.

We isolated adipose-derived MSC from C57BL/6 and CD1 mouse strains; as for human MSC, these cells gave rise to TMC with similar tumorigenic potential (data not shown).

Based on these results, we propose a two-step sequential model of spontaneous MSC immortalization and tumor transformation. The first step involves senescence bypass, which is infrequent in human cells (7); strikingly, all MSC samples bypassed this phase. In the second step, TMC cultures spontaneously acquire tumorigenic potential, although to date premalignant phenotypes have been described only for human adipose-derived MSC (16) and other cell types (10) after artificial immortalization by telomerase overexpression. Spontaneous transformation has not been previously reported for any human cell type.

In summary, we show that after long-term *in vitro* expansion, adipose tissue–derived human MSC populations can immortalize and transform spontaneously. This MSC-TMC transition could provide an *in vitro* model with which to study the origin and evolution of human cancers. MSC are being tested in clinical trials for tissue regeneration and engineering (17, 18), due to their plasticity, easy *ex vivo* expansion, and their presumed reduced risk for tumor formation compared with embryonic stem cells (19). Here we show that MSC maintained in prolonged culture may not be as risk-free as believed, supporting recent cautionary speculation that "mutant stem cells may seed cancer" (20). Specific cancer stem cells have been isolated, characterized, and defined in several human tumor types, including acute myeloid leukemia, glioblastoma, and breast cancer, and are proposed to derive from normal adult stem cells (1). Greater understanding of MSC biology is clearly needed to establish safe criteria for their potential clinical use.

Acknowledgments

Received 11/23/2004; revised 1/28/2005; accepted 2/7/2005.

Grant support: Plan Nacional de Salud y Farmacia CICYT grant SAF2001-2262 (A. Bernad), COST Action B19 "Molecular Cytogenetics of Solid Tumours" (J.C. Cigudosa), Spanish Ministry of Education and Science predoctoral fellowship (D. Rubio), MCYT and FIS postdoctoral scientist (J. Garcia-Castro), Spanish Council for Scientific Research (Department of Immunology and Oncology), and Pfizer (Department of Immunology and Oncology).

The costs of publication of this article were defrayed in part by the payment of page charges. This article must therefore be hereby marked *advertisement* in accordance with 18 U.S.C. Section 1734 solely to indicate this fact.

We thank I. Colmenero for histopathologic expertise; J.C. López for human adipose tissue samples; M. Ramírez, A. Alejo, and D. García-Olmo for critical discussions; and C. Mark for editorial assistance.

References

1. Pardal R, Clarke MF, Morrison SJ. Applying the principles of stem-cell biology to cancer. Nat Rev Cancer 2003;3:895–902.
2. Czyz J, Wiese C, Rolletschek A, Blyszczuk P, Cross M, Wobus AM. Potential of embryonic and adult stem cells *in vitro*. Biol Chem 2003;384:1391–404.
3. Pittenger MF, Mackay AM, Beck SC, et al. Multilineage potential of adult human mesenchymal stem cells. Science 1999;284:143–7.
4. Lloyd AC. Limits to lifespan. Nat Cell Biol 2002;4:E25–7.
5. Chin L, Artandi SE, Shen Q, et al. p53 deficiency rescues the adverse effects of telomere loss and cooperates with telomere dysfunction to accelerate carcinogenesis. Cell 1999;97:527–38.
6. Zuk PA, Zhu M, Mizuno H, et al. Multilineage cells from human adipose tissue: implications for cell-based therapies. Tissue Eng 2001;7:211–28.
7. Romanov SR, Kozakiewicz BK, Holst CR, Stampfer MR, Haupt LM, Tlsty TD. Normal human mammary epithelial cells spontaneously escape senescence and acquire genomic changes. Nature 2001; 409:633–7.
8. Lustig AJ. Crisis intervention: the role of telomerase. Proc Natl Acad Sci U S A 1999;96:3339–41.
9. Sedivy JM. Can ends justify the means?: telomeres and the mechanisms of replicative senescence and immortalization in mammalian cells. Proc Natl Acad Sci U S A 1998;95:9078–81.
10. Milyavsky M, Shats I, Erez N, et al. Prolonged culture of telomerase-immortalized human fibroblasts leads to a premalignant phenotype. Cancer Res 2003;63:7147–57.
11. Helman LJ, Meltzer P. Mechanisms of sarcoma development. Nat Rev Cancer 2003;3:685–94.
12. Secombe J, Pierce SB, Eisenman RN. Myc: a weapon of mass destruction. Cell 2004;117:153–6.
13. DePinho RA. The age of cancer. Nature 2000;408: 248–54.
14. Boukamp P, Petrussevska RT, Breitkreutz D, Hornung J, Markham A, Fusenig NE. Normal keratinization in a spontaneously immortalized aneuploid human keratinocyte cell line. J Cell Biol 1988;106:761–71.
15. Bergers G, Benjamin LE. Tumorigenesis and the angiogenic switch. Nat Rev Cancer 2003;3:401–10.
16. Serakinci N, Guldberg P, Burns JS, et al. Adult human mesenchymal stem cell as a target for neoplastic transformation. Oncogene 2004;23:5095–8.
17. Mangi AA, Noiseux N, Kong D, et al. Mesenchymal stem cells modified with Akt prevent remodeling and restore performance of infarcted hearts. Nat Med 2003;9:1195–201.
18. Horwitz EM, Gordon PL, Koo WK, et al. Isolated allogeneic bone marrow-derived mesenchymal cells engraft and stimulate growth in children with osteogenesis imperfecta: implications for cell therapy of bone. Proc Natl Acad Sci U S A 2002;99:8932–7.
19. Rosenthal N. Prometheus's vulture and the stem-cell promise. N Engl J Med 2003;349:267–74.
20. Marx J. Cancer research. Mutant stem cells may seed cancer. Science 2003;301:1308–10.